Version of Record: https://www.sciencedirect.com/science/article/pii/S0022024820300154
Manuscript_26d0f8784a6d4d888cf0cf64b16189bb

A study of in-situ etching of GaN in metalorganic chemical vapor deposition (MOCVD) by tertiarybutylchloride (TBCl)

Bingjun Li, Sizhen Wang, Mohsen Nami, and Jung Han*

Department of Electrical Engineering, Yale University, New Haven, CT 06520, USA

This paper reports a study of the effect of NH_3 flow rate and reactor temperature on the tertiarybutylchloride (TBCl) etching of patterned GaN-on-sapphire templates. It is found that a reduced NH_3 flow rate and an elevated reactor temperature can eliminate islands or dots on the surface, while at the same time, enhance the etching around dislocations. TBCl etching was also performed on planar bulk GaN templates with much lower dislocation density. We find an atomically flat and layer-by-layer etching behavior within the region free of dislocations. Surface kinetics analysis reveals a short diffusion length of etching products. Room-temperature photoluminescence (PL) and x-ray photoelectron spectroscopy (XPS) measurements confirm that TBCl etching is capable of removing the damage and impurities induced by plasma etching without introducing additional damage.

Keyword: A1. In-situ etching; B1. Tertiarybutylchloride (TBCl); A1. Surface characterization; A1. Surface kinetics; A3. Metalorganic chemical vapor deposition; B1. Nitrides

1. Introduction

Gallium Nitride (GaN)-based electronic devices have attracted considerable attentions due to its wide bandgap, large critical electric field and high electron mobility. In order to achieve the theoretical performance of GaN power devices, it is needed to develop selective area doping

* corresponding author email: jung.han@yale.edu

(SAD) technique of either p- or n-type to enable design flexibility and create lateral PN junction devices, including current-aperture vertical electron transistors (CAVETs) [1,2], junction-barrier Schottky (JBS) diodes [3,4], and superjunction (SJ) devices [5]. Ion-implantation and dopant diffusion have been widely used in Si- and SiC-based devices as SAD techniques [6,7]. However, these techniques are still under development for III-nitride-based devices due to intrinsic challenges in GaN material properties [8]. Selective-area growth (SAG) is a potential alternative to achieve selective doping for lateral junctions. Toward this goal a combination of selective area etching (SAE) followed by SAG is envisioned. Cl-based plasma etching or dry etching of GaN is widely used to create trenches and patterns of a high aspect ratio and side walls with smoothness and verticality [9]. However, plasma-induced damage introduces serious optical and electrical deteriorations [10,11]. Vapor-phase etching of GaN in metalorganic chemical vapor deposition (MOCVD) system, such as using H_2 and hydrogen chloride (HCl), have been reported before [12,13]. However, H_2 etching always introduces severe surface roughening, while HCl is highly corrosive and not compatible with MOCVD hardware.

Recently, we introduced a metal-organic (MO) precursor, tertiarybutylchloride (TBCl), which has been applied to other III-V material systems [14,15,16], into MOCVD system for GaN to remove the plasma-induced damage or replace the role of plasma etching [17]. TBCl is compatible with MOCVD operation and effective in achieving *in-situ* selective area etching (SAE) at reduced temperatures. We reported the etching chemistry and also demonstrated initially the ability to achieve generally smooth etching morphology. In this work we extended the TBCl etching to a broader range and also with additional parameters. We examined the atomistic-scale surface morphology to understand the etching kinetics. TBCl etching of GaN was

* corresponding author email: jung.han@yale.edu

also performed on bulk GaN substrates in comparison with etching on GaN-on-sapphire templates to ascertain the effect of dislocation-mediated etching. Atomic force microscopy (AFM) reveals a nearly ideal surface previously modeled by the Monte Carlo (MC) simulation [19], which in turn provides additional insights of the kinetics of surface dissociation, diffusion, and desorption with little step bunching [19]. A series of samples were prepared to examine the effect of dry-etching and TBCl-etching on the regrowth surfaces and interfaces. X-ray photoelectron spectroscopy (XPS) and photoluminescence (PL) provide strong evidence that *in-situ* TBCl etching can remove the plasma-induced damage or impurities without introducing additional damage.

2. Experimental

Two different types of GaN samples (which we term them "templates" below) were used in the TBCl-etching study. GaN epilayers on c-plane sapphire substrates, with a thickness of 2 µm and a dislocation density of around 10^9 cm^{-2}, were used in the initial exploratory study. Additionally, GaN homoepilayers on bulk GaN substrates, with a thickness of 1.5 µm and a dislocation density of around 10^6 cm^{-2}, were grown under nominally the same condition. Trimethylgallium (TMGa), TBCl, and NH_3 were used as precursors for Ga, Cl, and N, respectively. The growth for GaN took place at nominally 1030°C, under a reactor pressure of 200 mbar, with a flow of NH_3 at 2 standard liter per minute (slm) and a TMGa flow rate of 106 µmol/min. For the selective-area etching experiments, a 100 nm thick SiO_2 was deposited on GaN on sapphire samples by plasma-enhanced chemical vapor deposition (PECVD). Photolithography and reactive-ion etching (RIE) were used to pattern the SiO_2 and expose GaN within the openings. TBCl etching was performed on GaN-on-sapphire templates with various pattern sizes (e.g. 1 mm^2 opening, and stripe-

* corresponding author email: jung.han@yale.edu

patterned opening) at temperatures ranging from 800 to 860°C, with NH_3 flow rate in the 7 to 50 standard cubic centimeters per minute (sccm) range, and with constant 2.5 sccm of TBCl (7.71 μmol/min) and 6 slm of H_2, all for a duration of 15 mins. TBCl etching experiments were also performed on planar bulk GaN templates after the preliminary study of TBCl etching on GaN-on-sapphire templates. Four different etching processes were used on bulk GaN templates (Table I) in order to study the damage of dry etching and the effect of TBCl etching. Sample A is a bulk GaN template; Samples B, C, and D represent bulk GaN templates that were etched by dry etching, TBCl etching, and a combination of both, respectively. Sample D was first etched together with Sample B using plasma etching, and was etched by TBCl with Sample C after solvent cleaning. Scanning electron microscopy (SEM), atomic force microscopy (AFM), and an optical interferometric surface profiler (Zygo Nexview 3D Optical Profiler) were used to study the surface morphology of the samples. Room-temperature photoluminescence (PL) and x-ray photoelectron spectroscopy (XPS, PHI *VersaProbe* II Scanning XPS Microprobe) was performed on Sample A~D to study the surface quality and impurities, respectively. A 325nm HeCd laser was used as an excitation source for PL measurement.

Table I. Processes on Sample A~D.

	300nm plasma etching (80nm/min)	300nm TBCl etching (10nm/min)
Sample A		
Sample B	×	
Sample C		×
Sample D	×	×

3. Results and discussion

3.1 TBCl etching of patterned GaN-on-sapphire templates

* corresponding author email: jung.han@yale.edu

In the previous study of TBCl etching [17], we reported a trend of dependence of etching morphology on the partial pressure of NH_3, and we observed under SEM a high density of pyramidal islands or hillocks under high NH_3 flow rate or a high reactor pressure. Such etching features have been reported in the cases of InP [16], and were attributed to the presence of etching residuals on the surface due to their insufficient desorption rate, sometimes known as the "micro-masking effect", resulting in a local inhibition of etching process which generates these islands on the surface. By decreasing of reactor pressure and NH_3 flow rate, the desorption rate of the etching products was much enhanced; island-free SAE trenches were achieved at 800 °C and 50 mbar with 14 sccm of NH_3. In this work, we further explored the effect of temperature on the etching morphology (between 800 and 860°C), and we varied the NH_3 flow rate between 7 and 50 sccm while maintaining a constant flow rate of TBCl at 2.5 sccm using H_2 as the carrier gas, to study the etching behavior in greater detail. Fig. 1 shows the SEM images of the stripe patterns of GaN-on-sapphire templates after SAE by TBCl. At a high NH_3 flow (50 sccm) and a low temperature (800°C), corresponding to the upper left panel in Fig. 1, we observed a high density of pyramidal islands similar to what was reported earlier. With the increasing of reactor temperature and decreasing of NH_3 flow rate, the white islands/dots are greatly suppressed, while the surface morphology becomes rough with crater-like surface depressions or pits, corresponding to the bottom-right panel in Fig. 1. (The origin of these pits will be discussed shortly.) The trend of the suppression of white dots is consistent with our previous designation of these islands from the micro-masking effect due to the incomplete desorption of etching products; a higher temperature and lower NH_3 flow rate both help to increase the desorption and alleviate the micro-masking effect.

* corresponding author email: jung.han@yale.edu

AFM was performed on the same set of SAE samples to unveil the atomistic mechanisms during the in-situ etching. Images were taken specifically at the center of 1 mm^2 opening regions and are shown in Fig. 2. The white dots seen under SEM are now seen as protrusive islands randomly distributed on the atomic terraces delineated by jagged atomic steps. The size and density of the white dots, for example, reduced from 130 nm in height and ~10^9 cm^{-2} under 800°C and 50 sccm of NH_3, to 70 nm in height and 2 x 10^8 cm^{-2} under 830°C and same NH_3 flow rate. Under AFM, the depression seen in SEM are now resolved to be pits defined by concentric or spiral atomic steps having hexagonal contours. The density of the etching pits clearly depends on the etching condition, with the density varying from, for example, 3 x 10^7 cm^{-2}, when etched at 800 °C with 7 sccm of NH_3, to 3 x 10^8 cm^{-2}, at 860 °C with the same NH_3 flow rate. It is known that the vapor phase etching generally involves the preferential removal and desorption of surface atoms having more energetic configurations. We believe that a higher density of steps or active sites near the core of dislocations causes enhanced etching. Such phenomenon has been reported in Cl-based plasma or HCl vapor etching [10,11,18]. Also, as discussed in [17], a lower NH_3 flow rate will increase the surface coverage of Cl atoms, thus enhancing the etching around dislocations. Therefore, the overall rough background in Fig. 1 under the enhanced etching should be understood as a result of dislocation-mediated etching which is acerbated in the case of GaN on sapphire, having a dislocation density of around 10^9 cm^{-2}. In order to study and evaluate the surface or interface property without being affected by the high density of dislocations on sapphire, bulk GaN templates were subsequently used to compare and contrast with the GaN-on-sapphire samples.

3.2 TBCl etching of planar GaN templates

* corresponding author email: jung.han@yale.edu

Based on the above discussion, a planar bulk GaN template was etched with TBCl to ascertain the intrinsic etching morphology (Sample C). The etching condition was chosen to be 860 °C, 2.5 sccm of TBCl, 14 sccm of NH_3, and the etching time is 30 mins, which is expected to yield an etching depth of 300 nm. In Fig. 3, we compared the results from the GaN-on-sapphire template and bulk GaN template. Both of them were etched under the same condition but for halved etching time on GaN-on-sapphire template (15 mins). From the lower-magnification, 20 x 20 μm^2 scans [Fig. 3 (a) and (b)], one could clearly see a reduction of the density of etching pits, by about three orders of magnitude from ~2 x 10^8 cm^{-2} for GaN-on-sapphire templates [Fig. 3(a)] to 3 x 10^5 cm^{-2} for bulk GaN template [Fig. 3(b)]. A nearly 3 orders of magnitude reduction in etch pits densities correlates well with the estimated difference in the densities of dislocation between these two types of templates, providing a strong support of our hypothesis of enhanced etching around dislocations. We note that a detailed analysis of the morphology of TBCl etching on different types of dislocations is beyond the scope of this paper but will be reported later. Away from the region with dislocations, a step-flow pattern is maintained during the etching as shown in a zoomed-in 3 x 3 μm^2 scan [Fig. 3(d)]. The steps follow the miscut orientation to m-plane (~0.35°), with zig-zag or jagged step edges. The morphology bears great resemblance to simulated images of the thermal desorption of GaN using Monte Carlo (MC) method [19], where the key surface mechanisms include the detachment of atoms from specific sites on step edges, diffusion of atoms on terraces, desorption of atoms into the vapor phase, and the re-incorporation of atoms to adjacent step edges. The step morphology gives the tell-tale sign that the TBCl etching proceeds in a near-equilibrium manner dominated by surface processes facilitating the solid-to-vapor transition, in a way almost reciprocal to the vapor-to-solid transition in epitaxial growth.

* corresponding author email: jung.han@yale.edu

Based on the MC simulation, a key conclusion is the relative magnitude of the average terrace width (L_0) versus the diffusion mean-free path (x_s) for atoms on a terrace, defined as

$$x_s = \sqrt{\frac{D}{p_d}}$$

$p_d$is the desorption probability in the unit of inverse time, and D is the diffusion coefficient.

The ratio of these two parameters s, or s^2 according to Ref. 19,

$$s = \frac{L_0}{x_s}$$

was used to determine the degree of interaction among the roughly parallel atomic steps. A finer point we wish to make, in contrast to [19], the species that are at play in our etching experiments are likely to be the etching products, for example GaCl or $GaCl_3$. So, our discussion of surface kinetics including diffusion, desorption, and nucleation is not about the typical adatoms in epitaxy but the similar mechanisms of the reactant molecules. Continuing our discussion, when s^2 is less than 1, the diffusion mean-free path of the reactant molecules is greater than the terrace width due to a combination of a slow rate of desorption and/or a slow rate of nucleation [21], molecules can diffuse on the terrace to the adjacent step edges with low Schwoebel barrier and re-incorporate, making it possible for step bunching to happen. However, when s^2 is larger than one, atoms have short mean free path (enhanced desorption and/or nucleation), there is little communication among neighboring steps through surface diffusion. In this case large step bunching is inhibited and steps tend to stick in pairs with meandering step edges. From Fig 3(d), we tend to conclude that large step bunching is not observed on TBCl etched samples and less

* corresponding author email: jung.han@yale.edu

ordered step edges is presented, indicating that the diffusion length is relatively short, due to either a high desorption rate of Ga etching product or the nucleation rate.

As the in-situ TBCl etching is expected to be used in the regrowth of GaN for lateral junction devices, we proceeded to study the morphological, chemical, and optical properties of four samples prepared on bulk GaN templates. The detailed experimental design is listed in Table I. Fig. 4 shows the surface morphology under AFM and Zygo interferometric profiler for Sample A~D. The as-grown GaN template exhibits parallel and straight atomic steps [Fig. 4(a)]. After the plasma etching (Sample B), as shown in Fig. 4(b), atomic steps due to substrate miscut are no longer observable, indicating the presence of a strong component of physical etching. TBCl etching of as-grown GaN template [Sample C, Fig. 4(c)] has been discussed in details above and is included here for completeness. Finally, TBCl treatment of plasma-damaged surface (Sample D), generates high density of surface protrusions [Fig. 4(d)]. The origin of these protrusions should not be confused with the "white dot" we observed previously as shown in Fig. 3, since white dots are not observed on Sample C, which was etched side-by-side with Sample D by TBCl. In a preliminary way, we would assign these protrusions to the presence of Al contamination during the dry etching. Our argument is based on the fact that the etching chamber is made of Al and we found an Al peak, with a peak height of 2×10^{19} cm^{-3}, at the plasma-etched and regrowth interface by secondary ion mass spectroscopy (SIMS). As discussed in [13,20], HCl gas can hardly attack AlN while Cl_2 vapor is able to do so. Although at low NH_3 flow rate, the portion of Cl-radicals might increase compared to HCl, as explained in our previous work [17], the continuous flow of NH_3 during the etching might change the desorption of AlN. AlN, in this case, would serve as an etching mask to generate these protrusions. To complete the

* corresponding author email: jung.han@yale.edu

morphology study, we employed the interferometric optical profiler to survey Samples C and D over a large area (~90 μm x 90 μm). The profiler is able to resolve (sub)nanometer vertical depth and is useful in measuring the true depth of the dislocation-related etching pits. Both samples exhibit a generally flat background with a comparable density of etching pits. The depth of etch pits is around 90 nm for Sample C [Fig. 4 (e)], while it is 160nm for Sample D [Fig. 4 (f)]. Enhanced TBCl etching around dislocations for Sample D, the one first experienced dry etching, can be explained by the additional damage created by plasma etching. It has been reported that plasma etching generates N-vacancies or Ga-rich surface layers which tend to align or pile up along the dislocations [22,23]. Since Cl- or HCl attacks Ga-rich facets faster than N-rich ones [14,17], enhanced etching around dislocations can be observed on the sample with the plasma damage on the surface.

Lastly, PL [Fig. 5(a)] and XPS [Fig. 5(b)] have been applied to these four samples to study the optical and chemical properties at or below the GaN surfaces that have been subject to different processing procedures. Compared with the reference (as grown) Sample A, which has a distinct near band edge (NBE) emission intensity at room temperature, the dry etching (Sample B) leads to a complete disappearance of NBE signal at room temperature, in agreement with the report [10,11] of the plasma-induced surface and sub-surface damage. Subsequent TBCl etching on dry-etched surface leads to a full recovery of the NBE signal, indicating that the damage or impurities incurred by dry etching has been mostly removed (Sample D), and the TBCl etching alone does not generate much adverse effect (Sample C). XPS shows that dry etching causes an increase in the Cl peak, which can be removed by the TBCl etching. In this case, we note that XPS does not have enough sensitivity to detect the presence of Al which was revealed by SIMS.

* corresponding author email: jung.han@yale.edu

These two separate comparative studies offer additional support that TBCl can be used to remove the damage without introducing new defects, except the possible surface protrusions which are related to dry etching-related contamination.

4. Conclusion

In summary, it is found that NH_3 flow rate and reactor temperature have a profound influence on the surface morphology of etched surface. As the flow rate decreases and temperature increases, the islands on the surface are eliminated but etching of dislocation is enhanced. Atomic steps are observed after etching in the area free of dislocations on bulk GaN template. Surface kinetic analysis indicates a high desorption rate of Ga etching product or nucleation rate. Room-temperature PL and XPS results confirms the ability of TBCl to remove the plasma-induced damage and impurities while no damage is introduced by itself.

Acknowledgements

This work is supported by the Advanced Research Projects Agency-Energy (ARPA-E), U.S. Department of Energy, under Award Number DE-AR0000871 as part of the PNDIODES program managed by Dr. Isik Kizilyalli.

* corresponding author email: jung.han@yale.edu

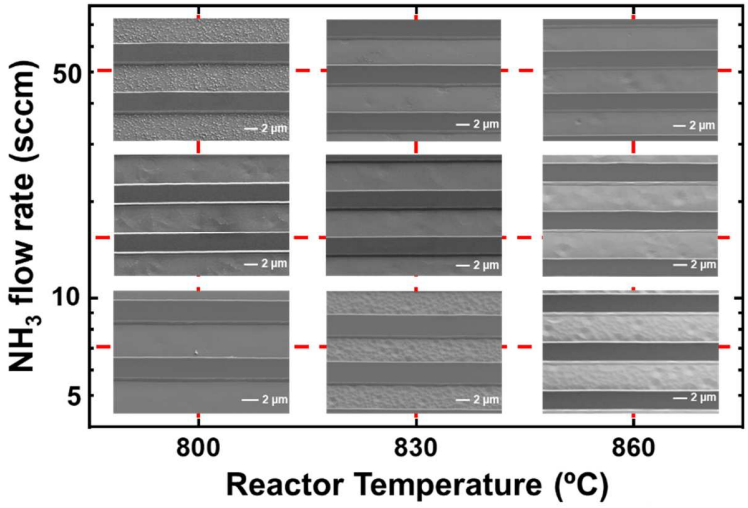

Fig. 1 30-degree tilted SEM images after selective area etching of GaN-on-sapphire templates with different NH_3 flow rate (7 ~ 50 sccm) and reactor temperature (800 ~ 860 °C) at a pressure of 50 mbar and 2.5 sccm of TBCl.

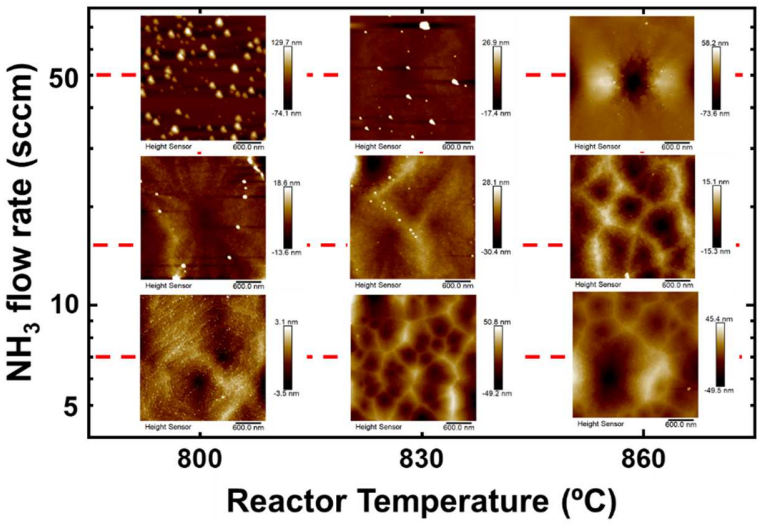

Fig. 2 Atomic force microscope (AFM) images (3 x 3 μm^2) at the center of 1 mm^2 opening patterns of GaN-on-sapphire templates after etching with different NH_3 flow rate (7 ~ 50 sccm) and reactor temperature (800 ~ 860 °C) at a pressure of 50 mbar and 2.5 sccm of TBCl.

* corresponding author email: jung.han@yale.edu

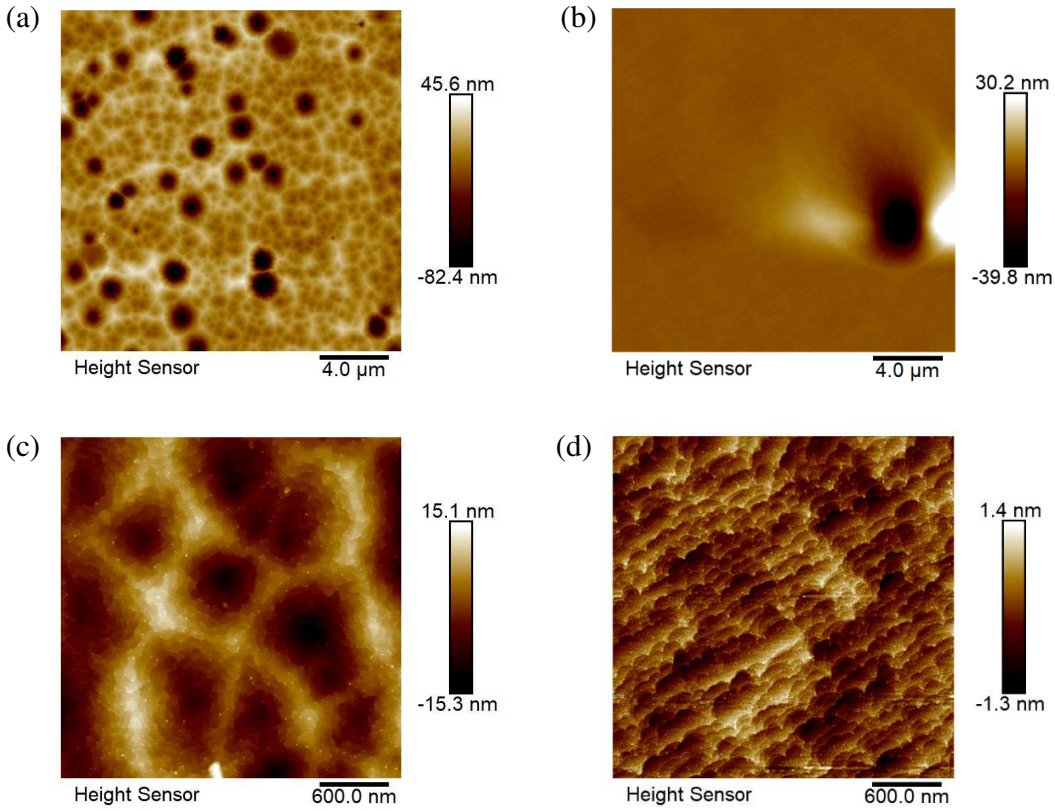

Fig. 3 AFM images of (a) 20 x 20 μm^2; (c) 3 x 3 μm^2 for GaN-on-sapphire template at the center of 1 mm^2 pattern after etching for 15min; and (b) 20 x 20 μm^2; (d) 3 x 3 μm^2 planar bulk GaN template after etching for 30min under the same condition, 860 ºC, 2.5 sccm of TBCl, and 14 sccm of NH_3 in H_2.

* corresponding author email: jung.han@yale.edu

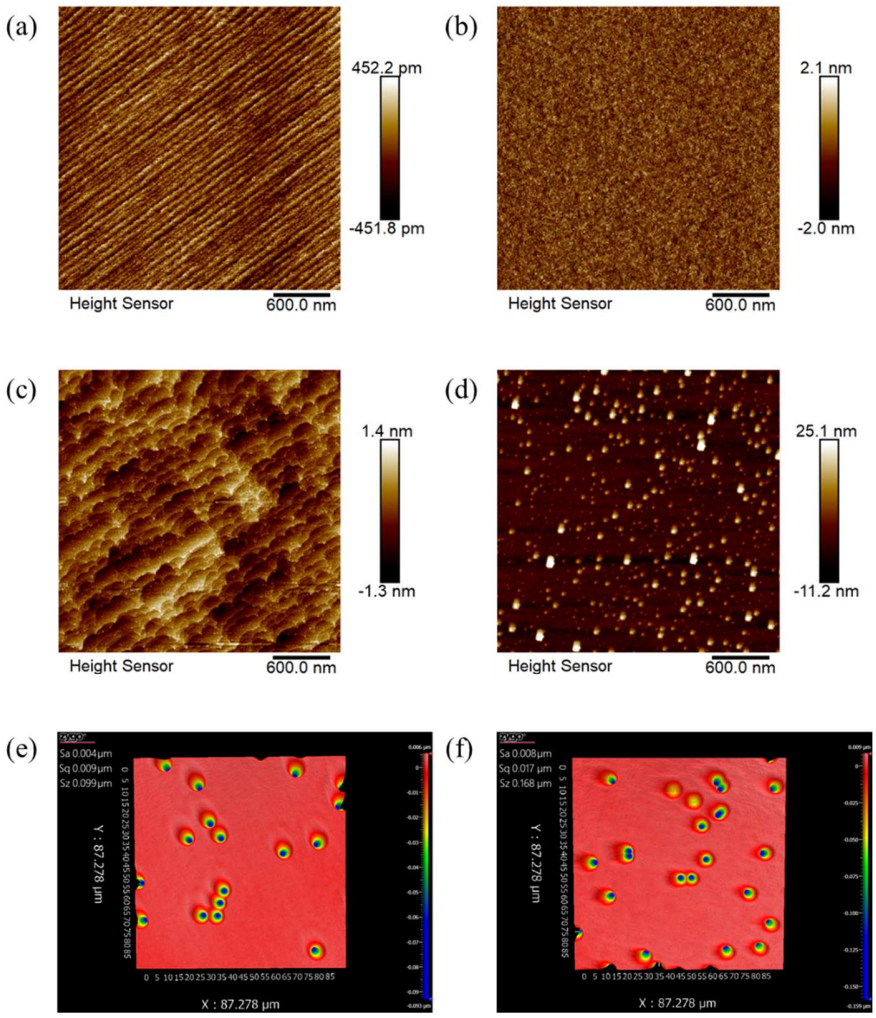

Fig. 4 3 x 3 µm^2 AFM images of (a) Sample A; (b) Sample B; (c) Sample C; and (d) Sample D. Zygo images of (e) Sample C, with pits depth of ~90nm; and (f) Sample D, with pits depth of ~160nm.

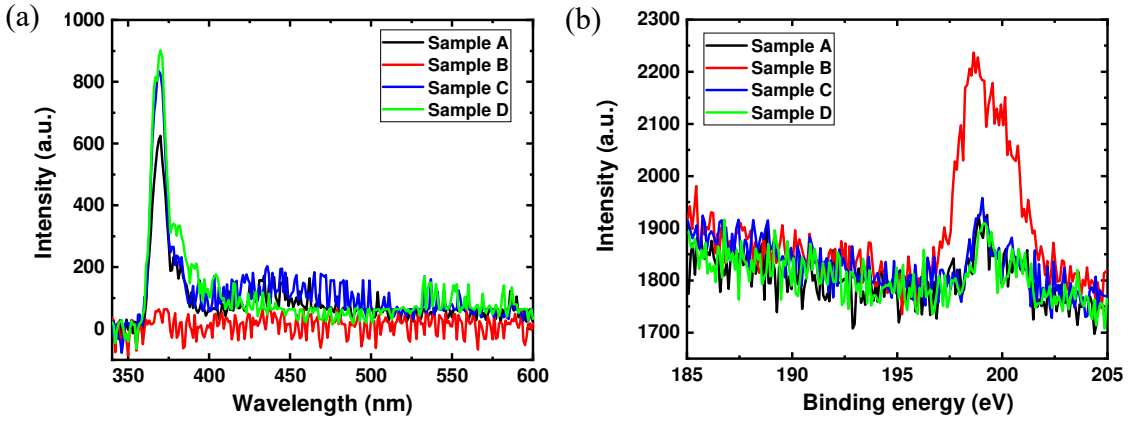

Fig. 5 (a) PL and (b) XPS of Cl 2p results on Sample A~D.

Reference

[1] I. Ben-Yaacov, Yee-Kwang Seck, Umesh K. Mishra, and Steven P. DenBaars, AlGaN/GaN current aperture vertical electron transistors with regrown channels, J. Appl. Phys. 95 (4) (2004) 2073-2078.

[2] Srabanti Chowdhury, Brian L. Swenson, and Umesh K. Mishra, Enhancement and Depletion Mode AlGaN/GaN CAVET With Mg-Ion-Implanted GaN as Current Blocking Layer, IEEE Electron Device Lett. 29 (6) (2008) 543-545.

[3] Ranbir Singh, Craig Capell, Allen R. Hefner, Jason Lai, and John W. Palmour, High-Power 4H-SiC JBS Rectifiers, IEEE Transactions on Electron Devices 49 (11) (2002) 2054-2063.

[4] Yuhao Zhang, Zhihong Liu, Marko J. Tadjer, Min Sun, Daniel Piedra, Christopher Hatem, Travis J. Anderson, Lunet E. Luna, Anindya Nath, Andrew D. Koehler *et al*., Vertical GaN Junction Barrier Schottky Rectifiers by Selective Ion Implantation, IEEE Electron Device Letters 38 (8) (2017) 1097-1100.

[5] Florin Udrea, Gerald Deboy, and Tatsuhiko Fujihira, Superjunction Power Devices, History, Development, and Future Prospects, IEEE Transactions on Electron Devices 64 (3) (2017) 713-727.

[6] James W. Mayer, Ion implantation in semiconductors, IEDM (1973).

[7] P. M. Fahey, P. B. Griffin, and J. D. Plummer, Point defects and dopant diffusion in silicon, Rev. Mod. Phys. 61 (2) (1989) 289-384.

[8] Kazunobu Kojima, Shinya Takashima, Masaharu Edo, Katsunori Ueno, Mitsuaki Shimizu, Tokio Takahashi, Shoji Ishibashi, Akira Uedono, and Shigefusa F. Chichibu, Nitrogen vacancies as a common element of the green luminescence and nonradiative recombination centers in Mg-implanted GaN layers formed on a GaN substrate, Appl. Phys. Express 10 (2017) 061002.

[9] R. J. Shul, G. B. McClellan, S. A. Casalnuovo, D. J. Rieger, S. J. Pearton, C. Constantine, C. Barratt, R. F. Karlicek, C. Tran, and M. Schurman, Inductively coupled plasma etching of GaN, Appl. Phys. Lett. 69 (8) (1996) 1119-1121.

[10] Zecheng Liu, Jialin Pan, Takashi Kako, Kenji Ishikawa, Keigo Takeda, Hiroki Kondo, Osamu Oda, Makoto Sekine, and Masaru Hori, Suppression of plasma-induced damage on GaN etched by a Cl2 plasma at high temperatures, Jpn. J. Appl. Phys. 54 (2015) 06GB04.

[11] Zecheng Liu, Jialin Pan, Atsuki Asano, Kenji Ishikawa, Keigo Takeda, Hiroki Kondo, Osamu Oda, Makoto Sekine, and Masaru Hori, Investigation of effects of ion energies on both plasma-induced damage and surface morphologies and optimization of hightemperature Cl2 plasma etching of GaN, Jpn. J. Appl. Phys. 56 (2017) 026502.

[12] D. D. Koleske, A. E. Wickenden, R. L. Henry, J. C. Culbertson, and M. E. Twigg, GaN decomposition in H_2 and N_2 at MOVPE temperatures and pressures, Journal of Crystal Growth 223 (2001) 466-483.

[13] D. Fahle, T. Kruecken, M. Dauelsbery, H. Kalisch, M. Heuken, and A. Vescan, In-situ decomposition and etching of AlN and GaN in the presence of HCl, J. Cryst. Growth, 393 (2014) 89-92.

[14] S. Codato, R. Campi, C. Rigo, and A. Stano, Ga assisted in situ etching of AlGaInAs and InGaAsP multi quantum well structures using tertiarybutylchloride, J. Cryst. Growth 282 (1-

* corresponding author email: jung.han@yale.edu

2) (2005) 7-17.
[15] Masahiko Kondow, Binqiang Shi, and Charles W. Tu, Chemical Beam Etching of GaAs Using a Novel Precursor of Tertiarybutylchloride (TBCl), Jpn. J. Appl. Phys., 38 (1999) L617-L619.
[16] D. Franke, N. Sabelfeld, W. Ebert, P. Harde, P. Wolfram, and N. Grote, Surface quality of InP etched with tertiarybutylchloride in an MOVPE reactor, J. Cryst. Growth, 248 (2003) 421-425.
[17] Bingjun Li, Mohsen Nami, Sizhen Wang, and Jung Han, In situ and selective area etching of GaN by tertiarybutylchloride (TBCl), Appl. Phys. Lett. 115 (2019) 162101.
[18] T. Hino, S. Tomiya, T. Miyajima, K. Yanashima, S. Hashimoto, and M. Ikedaa, Characterization of threading dislocations in GaN epitaxial layers, Appl. Phys. Lett. 76 (23) (2000) 3421-3423.
[19] Magdalena A. Załuska-Kotur, and Filip Krzyżewski, Step bunching process induced by the flow of steps at the sublimated crystal surface, J. Appl. Phys. 111 (11) (2012) 114311.
[20] Dirk Fahle, Investigation of HCl-assisted MOVPE of group III nitrides in a planetary hot-wall system, Ph.D. thesis, RWTH Aachen University (2014).
[21] JA Venables, Rate equation approaches to thin film nucleation, Philosophical Magazine 27 (3) (1973) 697-738.
[22] H K Cho, F A Khan, I Adesida, Z-Q Fang, and D C Look, Deep level characteristics in n-GaN with inductively coupled plasma damage, J. Phys. D: Appl. Phys. 41 (15) (2008) 155314.
[23] Z.-Q. Fang, D. C. Look, X.-L. Wang, Jung Han, F. A. Khan, and I. Adesida, Plasma-etching enhanced deep centers in n-GaN grown by metalorganic chemical vapor deposition, 82 (10) (2013) 1562-1564.

* corresponding author email: jung.han@yale.edu